

# Indonesian Physical Review

Volume 09 Issue 01, January 2026

P-ISSN: 2615-1278, E-ISSN: 2614-7904

## Magnetic Characteristics and Mineral Composition Analysis of Karst Rocks from Rammang-Rammang Karst Area, Maros Regency, South Sulawesi, Indonesia

Risda Syahruni<sup>1</sup>, Agus Susanto<sup>2</sup>, Muhammad Arsyad<sup>1</sup>, Subaer Subaer<sup>1</sup>, Husain Husain<sup>2,3\*</sup>

<sup>1</sup> Department of Physics, Postgraduate Program of Universitas Negeri Makassar, Indonesia.

<sup>2</sup> Department of Physics, Faculty of Mathematics and Natural Science, Universitas Negeri Makassar, Indonesia.

<sup>3</sup> Laboratory of Natural Materials and Magnetics, Department of Physics, Faculty of Mathematics and Natural Sciences, Universitas Negeri Makassar, Indonesia

Corresponding Author's E-mail: [husain.physics@unm.ac.id](mailto:husain.physics@unm.ac.id)

### Article Info

#### Article info:

Received: 18-09-2025

Revised: 18-12-2025

Accepted: 18-01-2026

#### Keywords:

Magnetic susceptibility;

VSM; XRF; XRD;

Rammang-Rammang

Karst

#### How To Cite:

R. Syahruni, A. Susanto, M. Arsyad, S. Subaer, and H. Husain, "Magnetic Characteristics and Mineral Composition Analysis of Karst Rocks from Rammang-Rammang Karst Area, Maros Regency, South Sulawesi, Indonesia", *Indonesian Physical Review*, vol. 9, no. 1, p 118-129, 2026.

#### DOI:

<https://doi.org/10.29303/iph.v9i1.575>.

### Abstract

This study investigates the magnetic characteristics and mineral composition of rocks in the Rammang-Rammang Karst area, Maros Regency, South Sulawesi, Indonesia, to clarify lithological variability and its implications for local magnetic anomalies. A total of 25 rock samples collected from field sampling points were analysed using a Bartington Susceptibility Meter, while five samples were further examined with a Vibrating Sample Magnetometer (VSM), X-Ray Fluorescence (XRF), and X-Ray Diffraction (XRD). The magnetic susceptibility values range from  $-0.6$  to  $10.5$   $m^3/kg$ , indicating a predominance of diamagnetic behaviour with minor contributions from paramagnetic and antiferromagnetic minerals. Hysteresis curve analysis from VSM confirmed the consistency between magnetic responses and susceptibility measurements. XRF results show that Ca dominates the rocks ( $>95\%$ ), with minor amounts of Fe, Ti, Si, Mn, Cu, Sr, Mo, In, and Co, as well as trace amounts of rare-earth elements (Lu, Eu). XRD analysis confirmed calcite ( $CaCO_3$ ) as the principal mineral phase, with crystallite sizes ranging from 39 to 44 nm, and the presence of dolomite in sample T18. The spatial distribution of magnetic susceptibility indicates that most of the study area exhibits low and negative values, reflecting diamagnetic behaviour. Whereas the highest value occurs at sampling point T12, which localizes the highest-susceptibility area, marked in red. These results indicate that the magnetic variability of Rammang-Rammang rocks is controlled by minor accessory magnetic minerals, providing valuable insights for mineral exploration and mitigating local magnetic anomalies.



Copyright (c) 2026 by Author(s). This work is licensed under a Creative Commons Attribution-ShareAlike 4.0 International License.

### Introduction

The Rammang-Rammang Karst Area is part of the Maros-Pangkep Karst region, which is the second-largest karst in the world, covering 46.200 hectares [1]. Rammang-Rammang Karst is located in Maros Regency and features a unique geological formation: a tower karst

geomorphology, formed by the dissolution of carbonate rocks in a tropical karst environment. This uniqueness has led to increased human activity in the area. One common activity in this area is the use of electronic devices, such as drones, for mapping or documentation [2].

The physical characteristics of rocks in the Rammang-Rammang Karst Area can influence the presence of magnetic minerals. These magnetic minerals can be found in rocks, soil, or sediment deposits [3]. Based on research on the physical properties of rocks in the Maros-Pangkep karst area, there are significant variations in density and porosity. The density of rocks in the Maros Karst Area ranges from 1.50 to 2.68 g/cm<sup>3</sup> and shows secondary porosity with values ranging from 0% to 50%. Meanwhile, rocks in the Pangkep Karst Area have a density ranging from 2.47 to 2.65 g/cm<sup>3</sup> and show primary porosity with values ranging from 0% to 5% [4]. These physical properties are related to fluid-rock interactions during secondary alteration processes and mineralization, which cause changes in rock composition, such as the addition of new minerals or the dissolution of existing minerals [5].

The Rammang-Rammang Karst area, which serves as a tourist destination, residential area, and research site, has led to widespread drone use by tourists, residents, and academics for various activities. The presence of magnetic minerals in this area has the potential to cause local magnetic field interference, affecting the use of magnetic field-based technology. Previous studies on magnetic properties in this area have only focused on guano deposits found in caves, which yielded magnetic susceptibility values ranging from  $278.0 \times 10^{-8}$  m<sup>3</sup>/kg to  $832.7 \times 10^{-8}$  m<sup>3</sup>/kg. These values are attributed to the accumulation of magnetic minerals derived from the surrounding rocks in the region [6]. However, to date, research specifically analysing the magnetic characteristics of rocks in the Rammang-Rammang Karst area remains very limited. In fact, data on rock magnetism and mineral composition are essential for mitigating potential local magnetic anomalies and as preliminary indicators of mineral resource potential.

The study of the magnetic characteristics of rocks can use various methods. One method that can be done is measuring the magnetic susceptibility value to determine the presence of magnetic minerals that may originate from human activities or naturally [7]. Measurement of magnetic susceptibility can indicate the extent to which rocks can be magnetized when exposed to an external magnetic field, and thus can be used to determine the content of magnetic minerals in the rocks [3]. Other environmental studies have successfully identified and mapped magnetic susceptibility values as an estimate of heavy metal contamination in soil by taking measurements using a Bartington magnetic susceptibility meter [8]. The study of magnetic characteristics can also be carried out using hysteresis curve analysis to determine more detailed magnetic parameters from the results of Vibrating Sample Magnetometer (VSM) measurements on samples [9]. The hysteresis curve from the VSM measurement results is also commonly used to determine the magnetic properties of iron sand in other studies that have been conducted [10]. Other research also uses VSM to identify the magnetic properties of silica-coated magnetite nanocomposites (Fe<sub>3</sub>O<sub>4</sub>/SiO<sub>2</sub>) synthesized from natural minerals [11].

In addition, to analyze the elemental content and mineral types in a rock sample in more detail, X-Ray Fluorescence (XRF) and X-Ray Diffraction (XRD) can be used, which can support rock magnetism studies. XRF is based on the identification and counting of X-rays produced from the photoelectric effect phenomenon to determine the elements in rocks, minerals, and

sediments[12]. Meanwhile, mineral type determination by XRD yields diffraction peak patterns at specific angles [13]. other study obtained  $\chi_{LF}$  values ranging from  $23.9 \times 10^{-8}$  m<sup>3</sup>/kg to  $2791.6 \times 10^{-8}$  m<sup>3</sup>/kg, with the presence of iron (Fe) and titanium (Ti) elements, as well as magnetic minerals such as magnetite (Fe<sub>3</sub>O<sub>4</sub>), hematite (Fe<sub>2</sub>O<sub>3</sub>), maghemite ( $\gamma$ -Fe<sub>2</sub>O<sub>3</sub>), and ilmenite (FeTiO<sub>2</sub>) from rock samples analyzed using XRF and XRD [7]. Other studies have also successfully used XRF and XRD analysis to determine the elemental and magnetic mineral content of iron ore and iron sand obtained from nature [13]. Therefore, the combination of these methods is highly relevant for studies on the magnetic characteristics and mineral composition of rocks.

Magnetic susceptibility data of the sample in the open field can also be used for spatial mapping of the magnetic susceptibility distribution in the area [14]. Magnetic susceptibility mapping shows variations in values at specific points, depending on the sampling points in the study. This mapping can be used as a basis for mineral exploration, geological mapping, and environmental studies [8]. In addition, information on rock magnetic characteristics provides a scientific baseline for understanding local magnetic variability, which is particularly relevant for magnetic field-based technologies because the presence of magnetic minerals can produce local magnetic anomalies. These anomalies can affect the performance of technologies that rely on magnetic-field-based navigation systems, such as drones with magnetic compasses, which are sensitive to local magnetic field disturbances. Information on the distribution of magnetic susceptibility and mineral composition of rocks in the Rammang-Rammang Karst Area is still limited. This research is necessary not only to support the reliable operation of magnetic field-based electronic devices, but also to be an initial indicator for the exploration of mineral resources with potential economic value in the area. Therefore, this research is important for filling data gaps and providing scientific information to various parties, including researchers, local governments, and industry players interested in the sustainable management and utilization of this unique karst landscape.

## **Experimental Method**

### **Rock Sampling and Preparation**

The sampling points consisted of 25 points determined based on the purposive sampling method, which is the selection of sampling locations based on specific considerations by researchers for various conditions in the study area [15]. Sampling locations were recorded using a Global Positioning System (GPS). The rock samples collected were fresh, unweathered limestone, not covered by soil, in accordance with geological sampling standards for geochemical analysis. Each sample was labeled according to its sampling point.

The collected rock samples were then cleaned, dried, and crushed. The samples were then sieved using a 100-mesh sieve [16]. The prepared samples were then weighed to the required mass: approximately 15 g for Bartington Magnetic Susceptibility Meter MS2B measurements, 1 g for VSM analysis, 5 g for XRF analysis, and 1-2 g for XRD analysis.

### **Characterizations**

Magnetic susceptibility measurements were performed on all 25 prepared samples using a Bartington Magnetic Susceptibility Meter with MS2B sensor and analyzed using Multisus software[3]. The measurements were conducted at the Geophysics Laboratory of Universitas

Halu Oleo. The magnetic susceptibility values obtained were then interpreted based on magnetic susceptibility classification by Dearing (1999) [17]. Five representative samples were selected based on the highest and lowest magnetic susceptibility values obtained from Bartington magnetic susceptibility meter measurements for further analysis using VSM, XRF, and XRD.

VSM measurements were performed at the Integrated Laboratory Unit of Universitas Negeri Malang using the PPMS VersaLab. These measurements were performed at room temperature with magnetic field variations ranging from  $-3$  T to  $3$  T. This VSM analysis produced a hysteresis curve or  $M$ - $H$  plot that was used to determine the saturation magnetisation ( $M_s$ ), remanent magnetization ( $M_r$ ), coercivity ( $H_c$ ), and magnetic susceptibility ( $\chi$ ) [9]. The magnetic susceptibility values were determined from the initial slope of the  $M$ - $H$  plot, calculated using [11]:

$$\chi_i = \left( \frac{dM}{dH} \right)_{H \rightarrow 0} \quad (1)$$

X-ray fluorescence is used to determine the quantitative composition of elements. [6]. XRF measurements were conducted at the Advanced Minerals and Materials Laboratory of Universitas Negeri Malang using PANalytical Minipal 4 XRF. The XRF instrument was calibrated using an aluminium standard with an operating voltage of  $14$  kV, a current of  $100$   $\mu$ A, and an input count rate of  $10000$  cps [18]. Elemental concentrations were reported in weight percent (%) or parts per million (ppm).

Mineralogical analysis was carried out using XRD [19]. These measurements were conducted at the Microstructure Laboratory of Universitas Negeri Makassar using an XRD instrument type Rigaku MiniFlex II, and performed in the  $2\theta$  range of  $5^\circ$ -  $90^\circ$  by recording the X-ray intensity at each angle. Mineral phases were identified by matching diffraction patterns with a reference database [6]. Crystallite size was estimated using the Scherrer equation [20]:

$$D = \frac{K\lambda}{\beta \cos \theta} \quad (2)$$

Where  $K$  is the shape constant ( $0.9$ ),  $\lambda$  is the X-ray wavelength,  $\beta$  is the full width at half maximum (FWHM), and  $\theta$  is the diffraction angle [21].

### Modelling the Magnetic Susceptibility Distribution Map

Magnetic susceptibility values from Bartington Susceptibility Meter measurements and GPS coordinates of the 25 sampling points were used to model the spatial distribution of rock magnetic susceptibility in the Rammang-Rammang Karst area. The susceptibility values were interpolated into contour maps using Surfer software [14],[22]. The data were then processed and visualized in ArcGIS to produce maps of magnetic susceptibility spatial variation across the study area.

## Result and Discussion

### Magnetic Characteristics of Rocks in Rammang-Rammang Karst Area

Table 1 shows the results of magnetic susceptibility measurements obtained with a Bartington low-frequency susceptibility meter.

**Table 1.** Magnetic Susceptibility Values Using Bartington Susceptibility Meter Measurements

Sample	Magnetic susceptibility ( $10^{-8} \text{ m}^3/\text{kg}$ )	Sample	Magnetic susceptibility ( $10^{-8} \text{ m}^3/\text{kg}$ )
T1	3.10	T14	-0.60
T2	0.50	T15	0.20
T3	0.80	T16	-0.50
T4	-0.50	T17	-0.40
T5	-0.20	T18	-0.60
T6	-0.10	T19	0.50
T7	-0.60	T20	-0.20
T8	-0.60	T21	-0.40
T9	-0.30	T22	-0.40
T10	-0.50	T23	-0.30
T11	-0.30	T24	-0.60
T12	10.50	T25	-0.60
T13	0.80		

The magnetic susceptibility values of rocks in the Rammang-Rammang Karst area, Maros, exhibit a considerable range, varying from  $-0.60 \times 10^{-8} \text{ m}^3/\text{kg}$  to  $10.50 \times 10^{-8} \text{ m}^3/\text{kg}$ . The variability of magnetic susceptibility in carbonate rocks may be influenced by the presence of minor amounts of secondary magnetic minerals. Samples with susceptibility values less than zero or negative values indicate diamagnetic, whereas T1, T2, T3, T12, T13, T15, and T19 with positive values indicate the paramagnetic or antiferromagnetic minerals of the rocks [3]. This category is based on Dearing's (1999) classification of susceptibility values.

Based on measurements obtained using the Bartington susceptibility meter, the highest magnetic susceptibility was recorded in sample T12. In contrast, most of the other samples displayed negative values, suggesting that the rocks are predominantly composed of non-magnetic minerals. The majority of samples fall within the diamagnetic and weak paramagnetic phases, with susceptibility values approaching those of pure calcite crystals, indicating low concentrations of impurities and magnetic minerals [3]. Samples T1, T12, and T13, which exhibit positive susceptibility values, as well as samples T14 and T18 with negative susceptibility values, were subsequently selected for VSM measurements.

### Mineral Composition of Rocks in Rammang-Rammang Karst Area

The carbonate rocks forming karst areas are generally composed of calcite, which may occur in both pure and impure forms. Impurities in calcite are caused by the presence of other elements [23]. Tables 2 and 3 show the XRF analysis results of rock samples from the Rammang-Rammang Karst area.

**Table 2.** Elements Composition of Rocks in Rammang-Rammang Karst Area Based on XRF Measurements

Sample	Elements (%)											
	Ca	Fe	Lu	Mn	Cu	Eu	Sr	Mo	Si	Ti	In	Co
T1	98.77	0.41	0.22	0.04	0.04	0.10	0.40	-	-	-	-	-
T12	98.75	0.54	0.18	0.05	0.04	0.20	-	0.27	-	-	-	-
T13	96.31	0.62	0.17	0.06	0.04	-	-	0.30	0.83	0.08	1.60	-
T14	99.15	0.23	0.15	0.06	-	-	-	0.30	-	-	-	0.11
T18	99.30	0.19	0.20	-	0.05	-	0.25	-	-	-	-	-

**Table 3.** Compounds Composition of Rocks in Rammang-Rammang Karst Area Based on XRF Measurements

Sample	Compounds (%)											
	CaO	Fe <sub>2</sub> O <sub>3</sub>	Lu <sub>2</sub> O <sub>3</sub>	MnO	CuO	Eu <sub>2</sub> O <sub>3</sub>	SrO	MoO <sub>3</sub>	SiO <sub>2</sub>	TiO <sub>2</sub>	In <sub>2</sub> O <sub>3</sub>	Co <sub>3</sub> O <sub>4</sub>
T1	98.99	0.39	0.17	0.03	0.03	0.09	0.31	-	-	-	-	-
T12	98.82	0.51	0.14	0.04	0.04	0.10	-	0.34	-	-	-	-
T13	95.83	0.58	0.13	0.05	0.03	-	-	0.38	1.50	0.08	1.40	-
T14	99.14	0.21	0.11	0.05	-	-	-	0.38	-	-	-	0.10
T18	99.43	0.18	0.15	-	0.04	-	0.20	-	-	-	-	-

The XRF results indicate that the rocks of the Rammang-Rammang Karst area are dominated by Ca, with concentrations exceeding 95.00%. Minor amounts of Fe, Ti, Co, and Si were detected, suggesting the presence of accessory minerals that influence the rocks' magnetic properties. Furthermore, trace amounts of Lu, Mn, Cu, Eu, Sr, Mo, and In were detected, indicating that the rocks contain impure calcite.

The primary oxide composition of the carbonate rock samples is CaO. Table 3 shows that CaO content ranges from 95.83% to 99.43%, confirming the dominance of calcite. The detection of Fe, primarily in the form of Fe<sub>2</sub>O<sub>3</sub>, represents a secondary magnetic mineral with antiferromagnetic characteristics formed during diagenetic processes [19]. Although the concentration of these magnetic minerals is relatively low, their presence may exert a measurable influence on the variability of the rocks' magnetic properties.

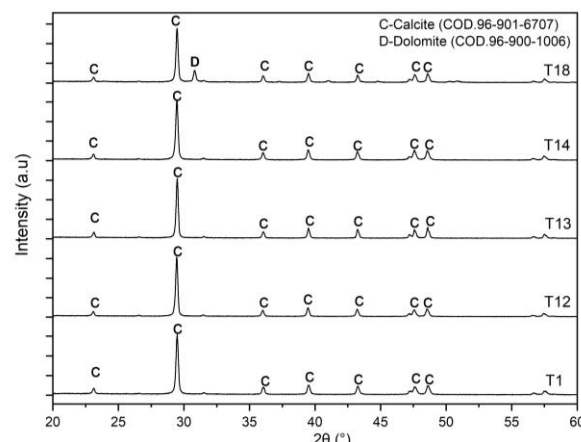


**Figure 1.** XRD measurement results of rock samples from Rammang-Rammang Karst Area

The XRD results for all samples exhibit a central diffraction peak at  $2\theta \approx 29.4^\circ$ , as shown in Figure 1. The dominant phase of the rock samples from the Rammang-Rammang Karst area is calcite ( $\text{CaCO}_3$ ) with a hexagonal crystal structure, based on the Crystallography Open Database (COD. 96-901-6707). The presence of this calcite phase dominates the entire diffraction pattern, confirming that calcite is the principal constituent of the karst rocks in the Rammang-Rammang area. In addition, Figure 1 reveals the presence of dolomite (COD. 96-900-1006) in sample T18, which represents another major constituent of the Maros karst rocks alongside calcite [24].

**Table 4.** XRD Analysis Results of Rocks in the Rammang-Rammang Karst Area

Sample	$2\theta$ (°)	Intensity (cps)	FWHM (°)	Crystal Size (nm)	Phase
T1	29.48	15736.67	0.21	39.59	Calcite
T12	29.44	20336.67	0.19	42.68	Calcite
T13	29.48	19710.00	0.18	44.19	Calcite
T14	29.46	16736.67	0.21	39.66	Calcite
T18	29.46	15553.33	0.19	42.22	Calcite

The crystallite sizes reported in Table 4 were calculated using the Scherrer equation, yielding values of 39.59–44.19 nm. These values indicate that the calcite in the samples is well crystalline. Carbonate rocks in Indonesia generally display sharp calcite diffraction peaks with crystallite sizes ranging from the nanometer to micrometer scale [25]. This finding is consistent with the XRF results, which show a high Ca content in the samples.

Magnetic mineral phases were not detected in significant amounts in the XRD results. This finding is consistent with the XRF analysis (Tables 2 and 3), which revealed only a small Fe content (<1%), indicating that the magnetic minerals present in the Rammang-Rammang Karst rocks occur predominantly as accessory phases. In natural carbonate rocks, the content of magnetic minerals is typically very low and is generally associated with transported magnetic particles from external environments or secondary alteration processes.

In addition, the presence of other rock-forming elements in the Rammang-Rammang Karst area (Tables 2 and 3), such as Mn as  $\text{MnO}$ , may influence the colouration of carbonate rocks, producing slightly brownish or pinkish hues. Non-carbonate compositions play a crucial role in determining rock color, as the adsorption of Fe and Mn often results in distinct color variations. The occurrence of Sr, with concentrations ranging from 0.20% to 0.40%, is commonly associated with diagenetic processes, where its presence indicates the involvement of ancient marine fluids during diagenesis and serves as an indicator of carbonate deposition in an aquatic environment [26]. This interpretation aligns with the geological history of the karst hills in this area, which originated from reef deposits in a shallow marine setting that progressively thickened, underwent cementation and compaction, and eventually formed a series of limestone hills [27].

Furthermore, rare earth elements (REEs), specifically Lu (Lutetium) and Eu (Europium), were also detected in concentrations of 0.10% to 0.20%. REEs encompass the lanthanide elements (La, Ce, Pr, Nd, Pm, Sm, Eu, Gd, Tb, Dy, Ho, Er, Tm, Yb, and Lu) along with Sc and Y [28]. The

presence of REEs in these carbonate rocks suggests the occurrence of rare minerals with potential applications in technological development [29].

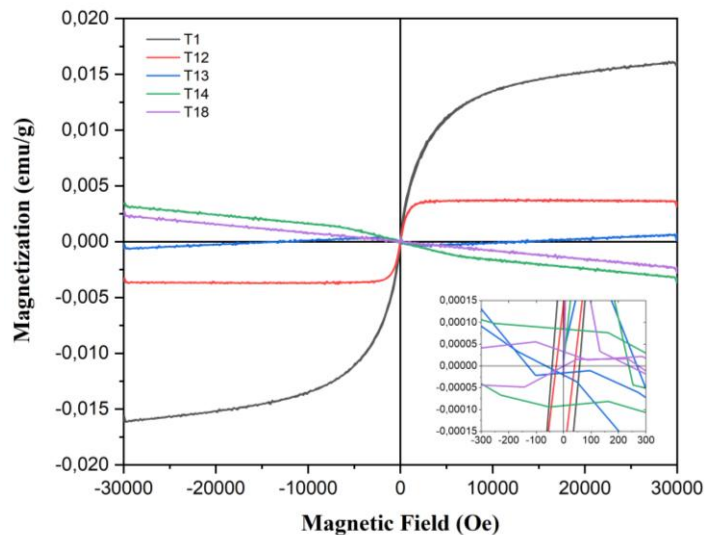


**Figure 2.** Room-temperature magnetic hysteresis (M-H) curves of samples T1, T12, T13, T14, and T18

Figure 2 is a combination of the hysteresis curves of samples T1, T12, T13, T14, and T18 from the VSM measurement results. This curve illustrates the relationship between magnetization ( $M$ ) and magnetic field ( $H$ ) of rock samples from the Rammang-Rammang Karst area measured at room temperature[30]. These hysteresis curves are consistent with the magnetic susceptibility values measured using the Bartington susceptibility meter. Samples T14 and T18 display very small gradients with negative slopes indicative of diamagnetism, consistent with their negative magnetic susceptibility values. Whereas T1, T12, and T13 produced different hysteresis loops that were not diamagnetic but indicated ferrimagnetic behaviour. Their positive slopes were consistent with their positive  $\chi$  values obtained from the Bartington magnetic susceptibility meter measurement. This suggests the possibility of a contribution from magnetic minerals that influence the sample's magnetic behavior. Hysteresis curve analysis yields magnetic parameters of the rock samples (Table 5), including variations in remanent magnetization ( $M_r$ ), coercivity ( $H_c$ ), and magnetic susceptibility ( $\chi$ )[11].

**Table 5.** Magnetic Parameters of Rocks in Rammang-Rammang Karst Area

Sample	Magnetic saturation	Magnetic remanence	Coercivity (Oe)	Magnetic susceptibility ( $10^{-8} \text{ m}^3/\text{kg}$ )	
	$(10^{-2} \text{ emu/g})$	$(10^{-3} \text{ emu/g})$		Bartington susceptibility meter	VSM
T1	1.60	0.33	41.60	3.10	9.10
T12	0.37	0.15	27.12	10.50	6.31
T13	0.07	0.04	266.33	0.80	0.20
T14	0.35	0.08	374.90	-0.60	-0.06
T18	0.28	0.03	359.28	-0.60	-0.27

The correlation between XRD and XRF results and magnetic properties suggests that the variation in measured magnetic susceptibility is primarily controlled by the presence of minor secondary magnetic minerals, such as iron oxides, alongside the dominant calcite phase. Carbonate rocks are typically diamagnetic, and only when iron-bearing minerals are present in sufficient amounts can their magnetic behaviour shift toward paramagnetism or ferrimagnetism. This interpretation is consistent with the magnetic susceptibility values, which are generally small and predominantly negative.

### Magnetic Susceptibility Distribution Map

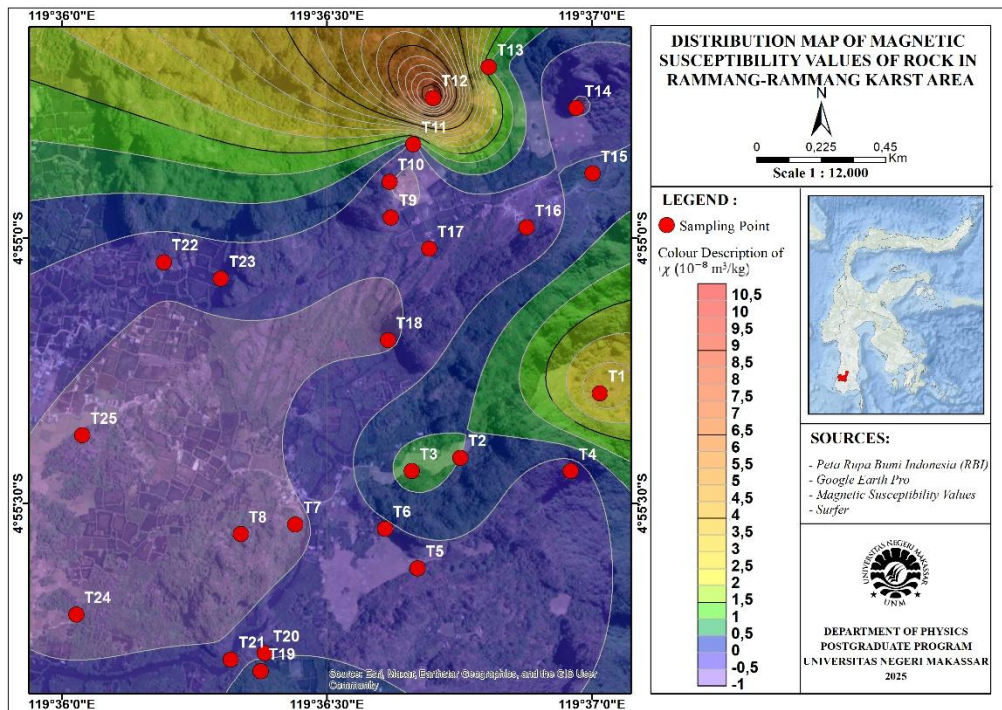


**Figure 3.** Magnetic susceptibility distribution map of rocks in Rammang-Rammang Karst Area

The spatial distribution map of magnetic susceptibility (Figure 3) illustrates the variation of  $\chi$  values across 25 sampling points in the Rammang-Rammang Karst area, based on measurements obtained using the Bartington susceptibility meter. The color gradient on the map reflects differences in magnetic susceptibility values, which are influenced by the concentration of magnetic minerals contained in the respective samples [8]. Most of the area exhibits negative magnetic susceptibility, as indicated by blue-to-purple color gradients, indicating diamagnetic behaviour.

The highest positive susceptibility value is localised at sampling point T12, indicated by a red-orange gradient. Points T1, T2, and T13 also show positive values, although at lower levels, marked by yellow-green gradients. These values suggest a higher hematite concentration than at the other sampling points. The spatial distribution map of  $\chi$  in the Rammang-Rammang Karst area thus provides an initial reference for the occurrence of accessory magnetic minerals in the karst environment. Areas with significant positive values, particularly around point T12,

may be prioritised for further mineral exploration. Moreover, this spatial information is relevant for mitigating potential local magnetic anomalies that could affect the performance of magnetically based navigation systems.

### Conclusion

This study provides an interpretation of the magnetic characteristics and mineral composition of rocks in the Rammang-Rammang Karst area. Combined results from magnetic susceptibility, hysteresis analysis, and mineralogical characterization show that the Rammang-Rammang karst area is dominated by carbonate rocks with diamagnetic behavior. Variations in magnetic response are controlled by minor accessory magnetic minerals. These findings indicate that although the magnetic mineral content is relatively low, its influence remains significant on local magnetic variations in a karst environment dominated by carbonate rocks. In relation to the research objectives, this study fills a data gap regarding the spatial distribution of magnetic susceptibility and mineral composition in the Rammang-Rammang Karst area. The results of this study have important implications for preliminary information of local magnetic anomalies that can support the operation of magnetic field-based technology, as well as an initial indicator of mineral resource potential, thereby supporting further geophysical research and sustainable management of the karst area in the region.

### Acknowledgment

The authors gratefully acknowledge the financial support provided by *DPPM through the PTM Research Scheme 2025* under contract number 2913/UN36.11/TU/2025, which made this study possible.

### References

- [1] A. Ahmad and A. S. Hamzah, *Database Karst Sulawesi Selatan*. Makassar: Badan Lingkungan Hidup Daerah Provinsi Sulawesi Selatan, 2016.
- [2] I. Agus Mandong, T. Budiarti, and A. Munandar, "Kajian Potensi Objek Daya Tarik Wisata Alam Karst Rammang-Rammang di Kabupaten Maros Provinsi Sulawesi Selatan," *J. Lanskap Indones.*, vol. 15, no. 1, pp. 36-41, Apr. 2023.
- [3] A. A., "Karakteristik Magnetik Tanah pada Lahan Produksi Kakao dan Jambu Mete Menggunakan Metode Suseptibilitas Magnetik," *J. Rekayasa Geofis. Indones.*, vol. 5, no. 01, pp. 14-23, Aug. 2023.
- [4] M. Arsyad, M. Rukmana, and P. Palloan, "Valuation of Physical Properties of Rocks in the Maros Pangkep Karst Area of Bantimurung Bulusaraung National Park," *J. Penelit. Pendidik. IPA*, vol. 8, no. 4, pp. 1954-1962, Oct. 2022.
- [5] A. A. Yarangga, "Keterdapatannya Alterasi Hidrotermal pada Daerah Wasegi (SP3) dan Sekitarnya Distrik Prafi Kabupaten Manokwari Propinsi Papua Barat," *INTAN J. Penelit. Tambang*, vol. 3, 2020.

- [6] A. Sambolangi, Subaer, A. Susanto, and M. Arsyad, "Analysis and extraction of mineral content from guano in karst and non caves," *Adv. Soc. Humanit. Res.*, vol. 2, no. 9, p. 16, 2024.
- [7] Hasria, M. R. Fiqriawan, S. Astuti, and Harisma, "Pemanfaatan Metode Kemagnetan Batuan di Indonesia," *Einstiens Res. J. Appl. Phys.*, vol. 2, no. 1, pp. 1–5, Feb. 2024.
- [8] S. R. Haraty, E. S. Hasan, and P. Melinda, "Pemetaan Nilai Suseptibilitas Magnetik Sebagai Pendugaan Pencemaran Logam Berat Pada Tanah Lapisan Atas Di Sepanjang Jalur Bypass Ranomeeto – Kendari Beach, Kota Kendari," *J. Rekayasa Geofis. Indones.*, vol. 5, no. 2, pp. 107–117, Agustus 2023.
- [9] R. Rinanda and D. Puryanti, "Analisis Sifat Magnetik Kalsium Ferit yang Disintesis Menggunakan Metode Metalurgi Serbuk," *J. Fis. Unand*, vol. 9, no. 2, pp. 224–230, Nov. 2020.
- [10] D. L. Puspitarum, G. Safitri, H. Ardiyanti, and M. S. Anrokhi, "Karakterisasi dan Sifat Kemagnetan Pasir Besi di Wilayah Lampung Tengah," *J. Pendidik. Fis.*, vol. 7, no. 2, p. 236, Sept. 2019.
- [11] H. Husain, R. Dewi, W. A. Adi, Y. Taryana, and S. Pratapa, "Structural analysis and magnetic-microwave absorption properties of natural mineral-derived silica-coated magnetite nanocomposites," *J. Magn. Magn. Mater.*, vol. 556, p. 169458, Aug. 2022.
- [12] S. Nono'o, R. Yunginger, G. H. Tamutuan, M. Demulawa, and I. Supu, "Identifikasi Jenis Mineral Magnetik Berdasarkan Uji XRF pada Sedimen Permukaan Sungai Bone di Daerah Pertambangan di Desa Tulabolo Timur, Suwawa, Kabupaten Gorontalo," *J. Nat. Sci.*, vol. 3, no. 2, pp. 1–7, Nov. 2023.
- [13] H. Husain, Y. Taryana, W. A. Adi, N. Nurhayati, M. Saleh, and N. Dewi, "Analisis X-Ray Flourescence dan X-Ray Diffraction Mineral Pasir dan Batu Besi Indonesia Sebagai Material Magnetik," *J. Sains Dan Pendidik. Fis.*, vol. 20, no. 1, p. 105, July 2024.
- [14] S. Alisna and S. Sinuraya, "Pemetaan Suseptibilitas Mmagnetik dan Penentuan Kandungan Logam pada Air Gambut di Kelurahan Tuah Madani Kecamatan Tampan Pekanbaru," *Komun. Fis. Indones.*, vol. 18, no. 1, pp. 12–17, Mar. 2021.
- [15] C. A. Aryanti, F. Amir, and I. Mishbach, "Distribusi Spasial Karbon Organik Total (KOT) dalam Sedimen di Perairan PLTU Tanjung Awar-Awar, Tuban, Jawa Timur," *J. Sains Dan Inov. Perikan.*, vol. 9, no. 1, pp. 118–124, 2025.
- [16] I. A. Sandi, M. Arsyad, and V. A. Tiwow, "Analisis Mineral Magnetik Guano Gua Kawasan Karst Maros Taman Nasional Bantimurung Bulusaraung," *J. Sains Dan Pendidik. Fis.*, vol. 20, no. 1, pp. 86–96, July 2024.
- [17] V. A. Tiwow, M. J. Rampe, and S. Sulistiawaty, "Suseptibilitas Magnetik dan Konsentrasi Logam Berat Sedimen Sungai Tallo di Makassar," *J. Ilm. SAINS*, vol. 22, no. 1, pp. 60–66, Apr. 2022.
- [18] F. Fahruddin, N. Haedar, A. Abdullah, A. Wahab, and R. Rifaat, "Deteksi Unsur Logam dengan XRF dan Analisis Mikroba pada Limbah Air Asam Tambang dari Pertambangan di Lamuru - Kabupaten Bone," *J. GEOCELEBES*, vol. 4, no. 1, pp. 7–13, Jan. 2020.

- [19] V. A. Tiwow *et al.*, "Estimation of mineralogical, morphological, and magnetic properties of the mineral sediments of guano caves in the karst area," *J. Chem. Technol. Metall.*, vol. 60, no. 2, pp. 275–285, Mar. 2025.
- [20] Z. Sinaga and J. Joniwarta, "Analisis Ukuran Kristal Dan Sifat Magnetik Melalui Proses Pemesinan Milling Menggunakan Metode Karakterisasi XRD, Mechanical Alloying, dan Ultrasonik Tekanan Tinggi pada Material Barium Hexaferrite (Bafe12o19)," *J. Kaji. Tek. MESIN*, vol. 5, no. 1, pp. 9–14, Apr. 2020.
- [21] M. Sumadiyasa and I. B. S. Manuaba, "Determining crystallite size using scherrer formula, Williamson-Hull plot, and particle size with SEM," *Bul. Fis.*, vol. 19, no. 1, p. 28, July 2018.
- [22] D. O. Oktavia, Salomo, and U. Malik, "Pemetaan Suseptibilitas Magnetik Endapan Tanah Sungai Sail Pekanbaru," *J. ONLINE Phys.*, vol. 4, no. 2, pp. 1–7, Sept. 2019.
- [23] Waode Jelita Ma'ruff Bay and Linda Pulungan, "Pemanfaatan Bahan Galian Mineral Kalsit Berdasarkan Karakteristik Sifat Fisik di Cikembar Sukabumi," *J. Ris. Tek. Pertamb.*, pp. 40–47, July 2022.
- [24] A. A. Rosari, A. Muris, and M. Arsyad, "Analisis Sifat Fisis dan Sifat Mekanik Batuan Karst Maros," *J. Sains Dan Pendidik. Fis. JSPF*, vol. 13, no. 3, pp. 276–281, Desember 2017.
- [25] E. Sulistiyo and A. Suharyanto, "Pengukuran Kristal Nano Magnesium Karbonat Dengan Metode X-Ray Diffraction (XRD)," *Semin. Nas. Sains Dan Teknol.* 2025, Mei 2025.
- [26] S. P. Putri, W. K. Hidajat, and R. Setyawan, "Studi Mikrofasies dan Diagenesis Batugamping Formasi Paciran, Desa Tegaldowo, Kecamatan Gunem, Kabupaten Rembang, Provinsi Jawa Tengah," *J. Geosains Dan Teknol.*, vol. 6, no. 2, pp. 104–120, Dec. 2023.
- [27] M. Ikhsan and H. Haris, "Ekowisata Rammang-Rammang Sebagai Laboratorium Pembelajaran Kontekstual Geografi di Kabupaten Maros," *JAMBURA GEO Educ. J.*, vol. 3, no. 2, pp. 43–51, Sept. 2022.
- [28] V. Balaram, "Rare earth elements: A review of applications, occurrence, exploration, analysis, recycling, and environmental impact," *Geosci. Front.*, vol. 10, no. 4, pp. 1285–1303, July 2019.
- [29] N. Rahmi, M. Arsyad, and A. Susanto, "Analisis Karakteristik Mineral Ornamen Gua Leang Lonrong Kawasan Karst Pangkep Sulawesi Selatan Taman Nasional Bantimurung Bulusaraung," *J. Fis. Flux*, vol. 19, no. 3, pp. 247–255, Oktober 2022.
- [30] R. Aprianto and K. S. Brtopuspito, "Analisis Suseptibilitas Magnetik Batuan Pengeboran di Blok Elang Sumbawa," *J. Pendidik. Fis. Dan Teknol.*, vol. 1, no. 3, pp. 226–234, Mar. 2017.